

CHAPTER 95

SCATTERING OF WATER WAVES BY VERTICAL CYLINDERS WITH A BACKWALL

Shohachi Kakuno *, Kazuki Oda*, and Philip L.-F. Liu **

Abstract

The scattering of small amplitude water waves by an array of vertical cylinders with a solid vertical backwall is studied theoretically and experimentally. In the theoretical study, a method of matched asymptotic expansions is developed without considering real fluid effects. The energy loss due to flow separation near cylinders is modeled by introducing a complex blockage coefficient. The theories are compared with laboratory data.

1 Introduction

The slit-type breakwater consists of a vertically slitted front wall and a solid backwall as shown in Figure 1. The closely spaced cylinders cause flow separation and hence energy dissipation. This type of device is particularly effective in reducing wave action inside a harbor. It has gained popularity in many countries, where either the materials for building rubble-mounted breakwaters are lacking or usable water space is limited. Many studies for the slit-type breakwater have been performed since Jarlan's original work(1961). Most recently a semi-analytical approach has been reported by Fugazza and Natale(1992).

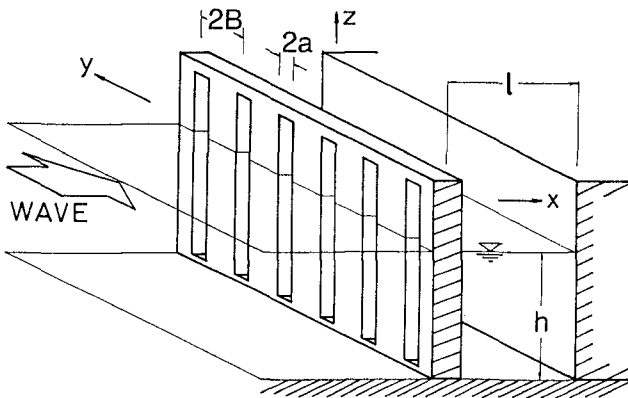


Figure 1. Slit-type breakwater.

*Dept. of Civil Engrg., Osaka City University, Osaka, 558, Japan.

**Joseph DeFrees Hydraulics Lab., School of Civil & Environmental Engrg., Cornell University, Ithaca, NY. 14853, USA.

The purpose of this study is to consider rigorously the mechanics of the interactions of water waves with the slit-type breakwater. The effects of the cross-section of the cylinders and energy dissipation caused by flow separation behind the cylinders are taken into consideration. The present work is the continuation of a previous study by Kakuno and Liu(1992) with additional consideration of the backwall.

2 Formulation of the Problem : Potential Flow Theory

A train of small amplitude monochromatic waves incidents normally upon an array of vertical cylinders with a vertical backwall. The distance between the centers of two adjacent cylinders is denoted as $2B$ and water depth is a constant h . The distance between the center line of the array of cylinders and the backwall, we call it wave chamber width hereafter, is denoted as l .

Ignoring the possibility of flow separation in the vicinity of the cylinders, a potential flow theory is first formulated. Defining the velocity potential for the periodic wave motion as

$$\Phi(x, y, z, t) = \phi(x, y) \frac{\cosh k(h+z)}{\cosh kh} e^{-i\omega t} \tag{2.1}$$

where ω is the wave frequency, and k the wave number which is the solution of the well-known dispersion relation

$$\omega^2 = gk \tanh kh. \tag{2.2}$$

The velocity potential on the still water level, $\phi(x, y)$, satisfies the Helmholtz equation

$$\nabla^2 \phi + k^2 \phi = 0, \tag{2.3}$$

in the flow domain with the no-flux boundary condition

$$\frac{\partial \phi}{\partial n} = 0, \tag{2.4}$$

on the perimeters of the cylinders and the backwall.

The incident waves propagate in the positive x -direction and their potential is expressed as

$$\phi_{inc} = e^{ikx}. \tag{2.5}$$

The scattered wave potential, which is the difference between the total wave potential ϕ and the incident wave potential, must satisfy the radiation boundary condition at infinity. The radiation boundary condition, which requires the scattered waves be outgoing at infinity, can be stated as

$$\phi - \phi_{inc} \rightarrow Re^{-ikx}, \quad \text{as } x \rightarrow -\infty \tag{2.6}$$

where R is the reflection coefficient.

In the region of the wave chamber, two types of waves exist : waves propagating in positive and negative x -direction. Thus,

$$\phi \rightarrow T e^{ikx} + Q e^{-ikx}, \quad \text{as } 0 \ll x < l \quad (2.7)$$

where T and Q are the ratios of amplitudes of these waves to that of the incident wave, respectively. If we apply the no-flux boundary condition on the front line of the backwall to these two waves, we obtain

$$Q = e^{2ikl} T. \quad (2.8)$$

3 A Method of Matched Asymptotic Expansions

To find analytical solutions for the velocity potential, ϕ , we develop a systematic procedure using a method of matched asymptotic expansions. First, the flow domain, $0 < y < B$, $-\infty < x < l$ is divided into two far-fields and a near-field. The near-field region is the flow domain in the vicinity of cylinders with the length scale of $O(B)$. The far-field regions are the flow domains far away from the cylinders, i.e. $O(|x|/B) \gg 1$, in which the length scale is the wave length. A method of matched asymptotic expansions is developed based on the assumption that $kB = \varepsilon \ll 1$.

3.1 Far-Field Solutions

If we match the far-field solutions and the near-field solution far away from cylinders, so that $O(|x|/B) \gg 1$ but $O(|kx|) \ll 1$, then evanescent modes can be discarded. In terms of the near-field coordinates $(\bar{x}, \bar{y}) = (x/B, y/B)$, (2.6) and (2.7) can be rewritten as:

$$\phi = e^{i\varepsilon\bar{x}} + R e^{-i\varepsilon\bar{x}}, \quad \bar{x} < 0 \quad (3.1a)$$

$$\phi = T e^{i\varepsilon\bar{x}} + e^{2ikl} T e^{-i\varepsilon\bar{x}}, \quad \bar{x} > 0. \quad (3.1b)$$

Expanding the reflection and the transmission coefficients in a power series of the small parameter ε , we have

$$R = \sum_{m=0}^{\infty} \varepsilon^m R_m, \quad (3.2a)$$

$$T = \sum_{m=0}^{\infty} \varepsilon^m T_m. \quad (3.2b)$$

Substituting (3.2) into (3.1), we obtain the inner expansions of the far-field solutions:

$$\begin{aligned} \phi \sim & (1 + R_0) + \varepsilon[R_1 + i(1 - R_0)\bar{x}] \\ & + \varepsilon^2 \left[R_2 - iR_1\bar{x} - \frac{(1 + R_0)\bar{x}^2}{2} \right] \\ & + \varepsilon^3 \left[R_3 - iR_2\bar{x} - \frac{R_1\bar{x}^2}{2} + \frac{i(R_0 - 1)\bar{x}^3}{6} \right] + \dots, \quad \bar{x} < 0 \end{aligned} \tag{3.3a}$$

$$\begin{aligned} \phi \sim & (1 + e^{2ikl})T_0 + \varepsilon[(1 + e^{2ikl})T_1 + i(1 - e^{2ikl})T_0\bar{x}] \\ & + \varepsilon^2 \left[(1 + e^{2ikl})T_2 + i(1 - e^{2ikl})T_1\bar{x} - \frac{(1 + e^{2ikl})T_0\bar{x}^2}{2} \right] \\ & + \varepsilon^3 \left[(1 + e^{2ikl})T_3 + i(1 - e^{2ikl})T_2\bar{x} - \frac{(1 + e^{2ikl})T_1\bar{x}^2}{2} - \frac{i(1 - e^{2ikl})T_0\bar{x}^3}{6} \right] \\ & + \dots, \quad \bar{x} > 0. \end{aligned} \tag{3.3b}$$

The reflection and transmission coefficients, R_m and T_m , are to be determined by matching (3.3) with the outer expansions of near-field solutions.

3.2 Near-Field Solutions

In the near-field the potential function is also expanded in a power series of ε , i.e.

$$\phi = \sum_{m=0}^{\infty} \varepsilon^m \phi_m. \tag{3.4}$$

In terms of the near-field coordinates (\bar{x}, \bar{y}) the governing equation, (2.3), can be rewritten as

$$\frac{\partial^2 \phi}{\partial \bar{x}^2} + \frac{\partial^2 \phi}{\partial \bar{y}^2} + \varepsilon^2 \phi = 0. \tag{3.5}$$

Substituting (3.4) into (3.5), we obtain a series of governing equations

$$\frac{\partial^2 \phi_m}{\partial \bar{x}^2} + \frac{\partial^2 \phi_m}{\partial \bar{y}^2} = 0, \quad m = 0 \text{ and } 1 \tag{3.6a}$$

$$\frac{\partial^2 \phi_m}{\partial \bar{x}^2} + \frac{\partial^2 \phi_m}{\partial \bar{y}^2} + \phi_{m-2} = 0, \quad m = 2, 3, 4, \dots \tag{3.6b}$$

The boundary condition requires that the no-flux condition be satisfied for all ϕ_m , i.e. $\partial\phi_m/\partial n = 0$ ($m = 0, 1, 2, \dots$) along solid surfaces.

The solution of the Laplace equation and the homogeneous solutions of Poisson equation can be interpreted as a uniform flow passing an opening in a channel. The dimensional velocity potentials for the uniform flow, ϕ' , can be written asymptotically as

$$\phi' \sim U'(x \pm C') + F' \quad x \gtrsim 0 \quad (3.7)$$

in which U' is the velocity intensity, F' is an arbitrary constant and C' is the blockage coefficient. The blockage coefficient depends on the geometry of the cylinder and is independent of the wave characteristics. A brief discussion on the blockage coefficient for the circular and rectangular cylinders is given in Kakuno and Liu(1992). Rewriting (3.7) in a dimensionless form in terms of the near-field coordinates, we have

$$\phi \sim U \left(\bar{x} \pm \frac{C}{\varepsilon} \right) + F, \quad \bar{x} \gtrsim 0 \quad (3.8)$$

in which

$$C = kC' \quad (3.9)$$

is the dimensionless blockage coefficient and is of order of magnitude of one or smaller. The scales in (3.8) and (3.9) are used so that the dimensional blockage coefficient, C' , can become large when the opening of the gap is small in comparison with the distance between two cylinders.

The velocity intensity U and the constant potential F are also expanded in terms of the small parameter, ε , i.e.

$$U = \sum_{m=0}^{\infty} \varepsilon^m U_m, \quad F = \sum_{m=0}^{\infty} \varepsilon^m F_m. \quad (3.10)$$

Substitution of (3.10) into (3.8) yields the outer expansions of the near-field potentials which are the solution of the Laplace equation.

3.3 Matching

After matching the far-field solutions of the leading order with the near-field solutions of the same order, the leading order coefficients may be obtained. The subsequent order coefficients may be calculated from the perturbation scheme with the known coefficients of the preceding order, that is,

$$U_0 = 0, \quad (3.11a)$$

$$F_0 = \frac{1 - iC(1 - e^{2ikl}) + e^{2ikl}}{1 - iC(1 - e^{2ikl})}, \quad (3.11b)$$

$$T_0 = \frac{1}{1 - iC(1 - e^{2ikl})}, \quad (3.11c)$$

$$R_0 = \frac{-iC(1 - e^{2ikl}) + e^{2ikl}}{1 - iC(1 - e^{2ikl})}, \quad (3.11d)$$

$$U_1 = i(1 - e^{2ikl})T_0, \quad (3.12a)$$

$$F_1 = \frac{-iM(iC - e^{2ikl} - 1)}{1 - iC(1 - e^{2ikl})}F_0, \quad (3.12b)$$

$$T_1 = \frac{(i + C)M}{1 - iC(1 - e^{2ikl})} F_0, \tag{3.12c}$$

$$R_1 = \frac{i[(1 + e^{2ikl}) - iC(1 - e^{2ikl})]M}{1 - iC(1 - e^{2ikl})} F_0, \tag{3.12d}$$

$$U_2 = \frac{e^{2ikl}M}{1 - iC(1 - e^{2ikl})} F_0, \tag{3.13a}$$

$$F_2 = \frac{(1 + e^{2ikl})T_2 + R_2}{2}, \tag{3.13b}$$

$$T_2 = \frac{(i + C)M}{1 - iC(1 - e^{2ikl})} F_1, \tag{3.13c}$$

$$R_2 = \frac{[i + C - (C - i)e^{2ikl}]M}{1 - iC(1 - e^{2ikl})} F_1, \tag{3.13d}$$

where $2M$, a net flux across the surface of the cylinder generated to compensate the flux by a symmetric part of the particular solution of the Poisson equation, is determined by

$$2M = - \int_{\Gamma} \frac{\partial}{\partial n} \left(-\frac{\bar{x}^2}{2} \right) ds = -\frac{S}{B^2} \tag{3.14}$$

where \vec{n} is pointing outward from the fluid region, Γ is the surface of the cylinder, and S is the half of the cross sectional area of the cylinder.

3.4 Reflection Coefficient

Up to the $O(\varepsilon^2)$ the reflection coefficient can be expressed as

$$R = R_0 + \varepsilon R_1 + \varepsilon^2 R_2. \tag{3.15a}$$

The absolute value of the reflection coefficient of leading order is unity, which fulfill the energy conservation, regardless of the wave characteristics, the wave chamber width, and the porosity of the front wall, or C . The whole solution which includes higher-order terms, therefore, does not satisfy the energy conservation principle. In particular, the deviation of that solution from the principle become significant in the vicinity of region of $l/\lambda = 0.5$, where λ is the wave length.

3.5 Free surface displacement inside and outside the wave chamber

For design purpose, the free surface displacement in front of and behind the front wall, and in front of the backwall should be predicted. Knowing the phase difference in the free surface displacement inside and outside the wave chamber is helpful to get insight into the wave mechanics around the breakwater.

From the linear wave theory the free surface displacement can be related to the velocity potential Φ through the free surface boundary condition

$$\eta = \Re e \left[-\frac{1}{g} \frac{\partial \Phi}{\partial t} \right]_{z=0} \quad (3.16)$$

Substituting (2.1) into the above equation and collecting the real part of the resulting equation, we obtain

$$\eta = \frac{\omega}{g} \sqrt{\alpha^2 + \beta^2} \sin \left[\omega t + \tan^{-1} \frac{\alpha}{\beta} \right] \quad (3.17)$$

where

$$\alpha = -\Im m[\phi(x, y)], \quad (3.18a)$$

$$\beta = \Re e[\phi(x, y)]. \quad (3.18b)$$

The phase difference in the free surface displacement inside and outside the wave chamber is, therefore,

$$\theta = \tan^{-1}(\alpha_O/\beta_O) - \tan^{-1}(\alpha_I/\beta_I) \quad (3.19)$$

where the subscript "O" and "I" stand for "outside" and "inside" of the wave chamber.

4 Energy Dissipation Model

As shown in (3.7) the outer expansions of the near-field solutions represent uniform flows with a difference in potential level. This difference denoted by the blockage coefficient, C' , can be related to the pressure drop between the front and the rear of the front wall. In the dimensional form, the dynamic pressure is defined as

$$P = -\rho \frac{\partial \Phi}{\partial t} = i\rho\omega\phi(x, y) \frac{\cosh k(h+z)}{\cosh kh} e^{-i\omega t}. \quad (4.1)$$

Substituting (3.7) into the above equation, we obtain the dynamic pressures in front of and behind the wall

$$P = i\rho\omega[U'(x \pm C') + F'] \frac{\cosh k(h+z)}{\cosh kh} e^{-i\omega t}, \quad x \gtrless 0 \quad (4.2)$$

If we neglect terms whose order are higher than $O(k^2)$, the pressure difference between P_+ and P_- is

$$\Delta P = P_- - P_+ = 2\rho C' \dot{U} \quad (4.3)$$

where

$$\dot{U} = \frac{dU}{dt}; \quad U = U' \frac{\cosh k(h+z)}{\cosh kh} e^{-i\omega t}. \quad (4.4)$$

Therefore, the blockage coefficient C' plays a role of a coefficient of inertia resistance which is proportional to the acceleration of the oscillating flow U , (4.4).

To include the effects of energy dissipation due to flow separation in front of and behind the front wall, we assume that the flow separation is confined within the near field region. We assume that the energy dissipation causes an additional pressure drop, which is linearly proportional to the oscillating velocity U . Thus

$$\Delta P = 2\rho C' \dot{U} + 2\rho C'_i \omega U \tag{4.5}$$

in which C'_i can be considered as an empirical coefficient modeling the effects of energy dissipation. The simple model (4.5) can be derived in a different way. We introduce the blockage coefficient C' in (4.2) as a complex constant, i.e.

$$C' = C'_r + iC'_i \tag{4.6}$$

so that C'_r is the actual blockage coefficient based on the potential flow theory. Substituting (4.6) into (4.2), we can derive (4.5) with C' being replaced by C'_r . The significance of the simple relations stated in (4.5) and (4.6) is that when the energy dissipation is important, one can calculate the reflection coefficient (3.15) by replacing C by C' .

It is well known that the energy loss due to the flow separation is proportional to the square of the flow velocity through the opening, i.e.

$$\frac{\Delta P}{\rho g} = f' \frac{V^2}{2g} \tag{4.7}$$

where f' is the energy loss coefficient and V is the average velocity at the opening ($x = 0$). Because the dissipation model introduced in (4.5) is linear in the velocity field, we must ensure that the same total energy loss (work done) over a wave period is determined by the quadratic resistance law and by the linear model. By equating the work done (energy loss) calculated from the linear model and the one calculated from quadratic resistance law, we get

$$\frac{C'_i}{B} = \frac{|\tau|(H/\lambda)f}{9\pi/4 (a/B)^2 (B/\lambda)} \left[\frac{\sinh^2 kh + 3}{\sinh 2kh + 2kh} \right] \tag{4.8}$$

and

$$f = f' \gamma \tag{4.9}$$

in which "a" denotes the half-width of the opening, "H" is the incident wave height, γ is an empirical coefficient, and τ is the ratio of the uniform velocity far away from the cylinder to the water particle velocity of the incident wave at the same position, and expressed as

$$\tau = (1 - e^{2ikl})T. \tag{4.10}$$

Equation (4.8) relates C'_i to the wave characteristics, H/λ , τ , kh , and the geometry of the cylinder, a/B and B/λ . Only one dimensionless coefficient, f , need to be determined. The value of f may hold the same as that for the case without the backwall, say, 1.5 for rectangular cylinders.

5 Comparison Between Theoretical Solutions and Laboratory Data

To validate the theoretical models with the value of $f = 1.5$ for rectangular cylinders, experimental data obtained in Osaka City University are compared with theoretical results.

The cylinders used are square. The experiments are performed in a wave tank, which is 1.0m wide, 50m long and 1.75m deep. The side lengths of the square cylinders are 15cm for the case of $B/l = 0.129$ and 5cm for other cases. The water depth is kept constant at $h = 50\text{cm}$. The wave steepness H/λ varies slightly around 0.01. The wave heights are measured in front of and behind the front wall and in front of the backwall.

From Figure 2(a) to Figure 2(d), the laboratory data for the reflection coefficients are compared with the theoretical results obtained for $f = 1.5$, for different parameters, a/B (porosity), B/l , and h/B . The theoretical results obtained from the leading term only and from higher-order terms are shown in the figures. The discrepancy between these two types of the results is slight except the region of $l/\lambda = 0.5$ where the higher-order solutions exhibit singular behavior. The agreement between data and theoretical results from the leading term only is good so that it is suffice for practical use to employ only the leading term. In Figure 3, the all experimental data of the reflection coefficients are plotted against the theoretical results. Both are in good agreement except for the region where the values are close to unity.

Figure 4 shows an example of the comparison in the free surface displacements at three locations inside and outside the wave chamber. The vertical displacements are normalized by the incident wave amplitude. Figure 5 plots the phase difference between the locations inside and outside the chamber. Both figures are the results based on the leading order approximation. The locations at which the free surface displacements are measured are indicated in the captions of each figure. The agreement between data and theory is again good for these results. Note that nodes appear behind the cylinders at a definite value of l/λ . Sudden jumps shown in the phase difference, which is about π , are because that the location of the wave gauge behind the cylinder (x_2) is in the vicinity of a nodal point.

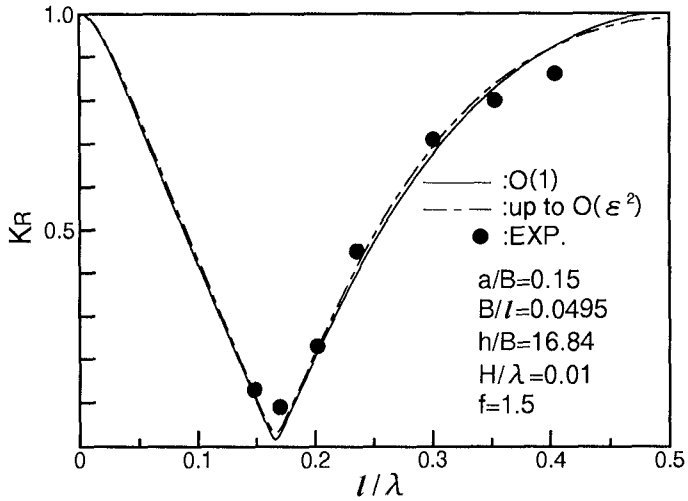


Figure 2(a). Comparison between theoretical and experimental data for reflection coefficient.

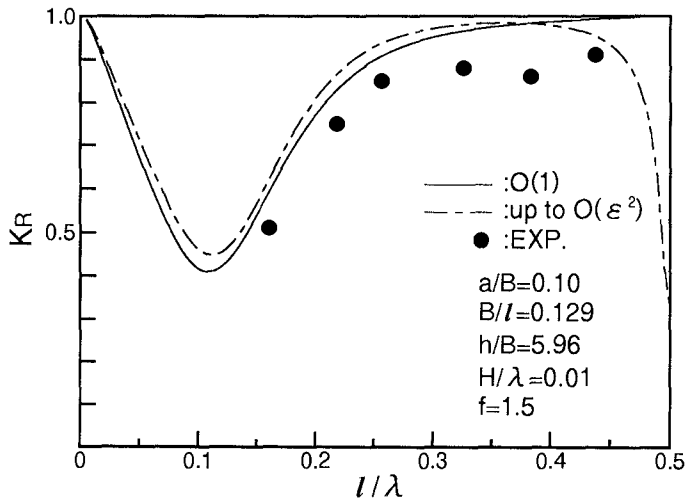


Figure 2(b). Comparison between theoretical and experimental data for reflection coefficient.

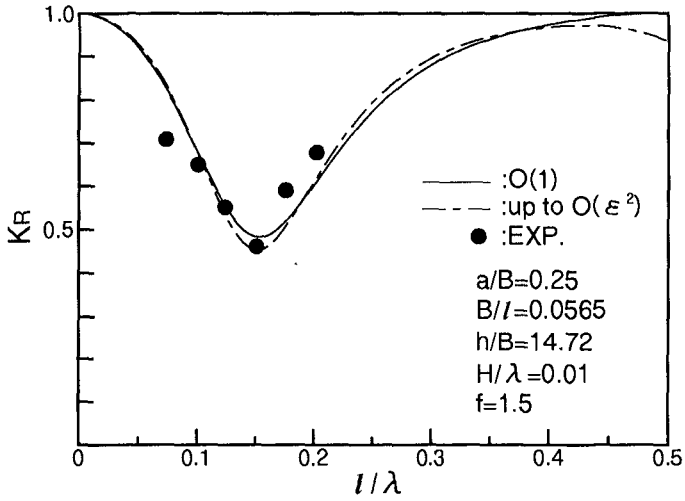


Figure 2(c). Comparison between theoretical and experimental data for reflection coefficient.

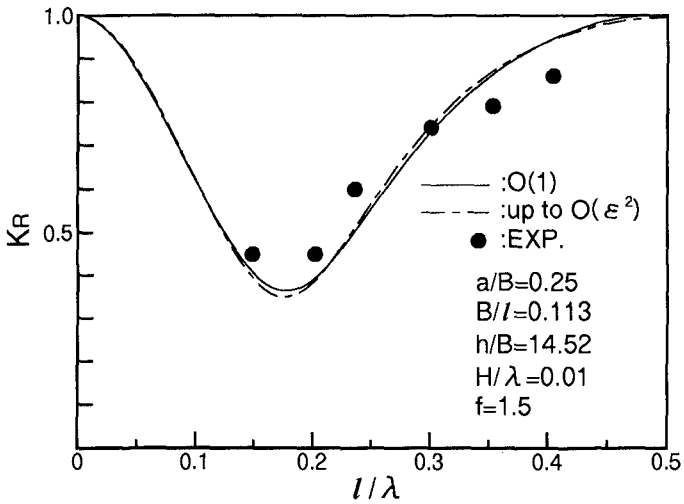


Figure 2(d). Comparison between theoretical and experimental data for reflection coefficient.

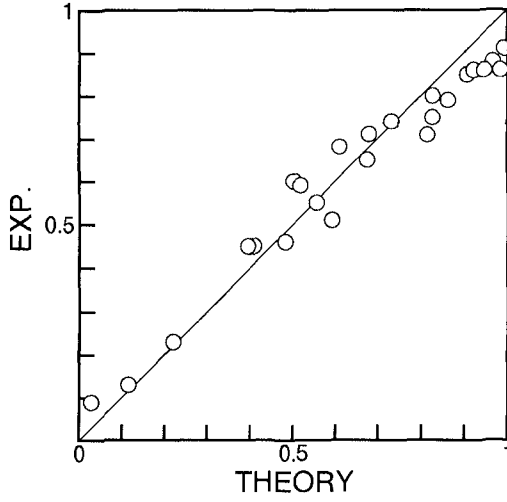


Figure 3. Comparison between measured and calculated reflection coefficients.

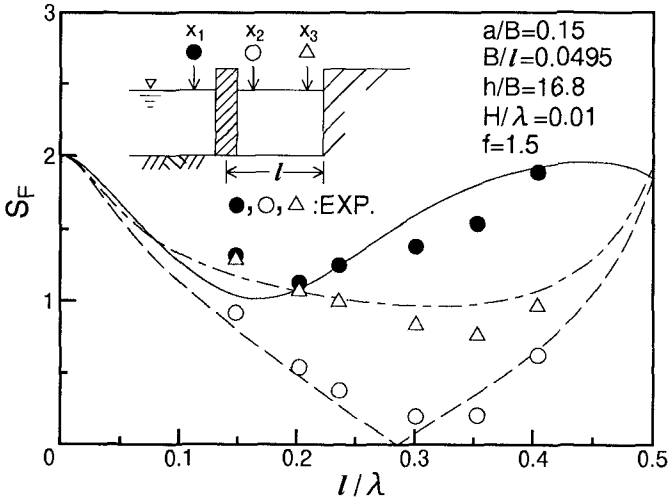


Figure 4. Comparison between theoretical and experimental data for free surface displacements, $x_1/l = -0.125$, $x_2/l = 0.125$, $x_3/l = 0.917$.

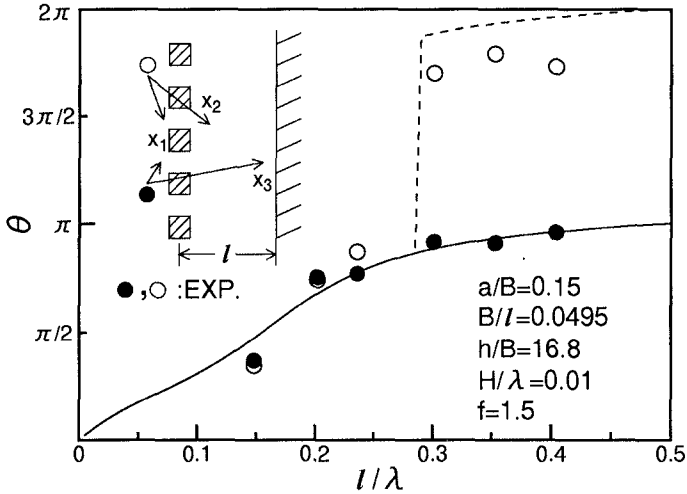


Figure 5. Comparison between theoretical and experimental data for phase differences between inside and outside the chamber, $x_1/l = -0.125$, $x_2/l = 0.125$, $x_3/l = 0.917$.

6 Conclusion

A modified method of matched asymptotic expansions has again been applied to study the wave interactions with a slit-type breakwater. The energy dissipation caused by the flow separation behind the cylinders is considered in the theory. Theoretical results with the empirical coefficient for square cylinders determined in the previous study are verified by experimental data. It is shown that the leading order solutions are accurate and can be used to calculate reflection coefficients and the wave action in the vicinity of the breakwater.

7 Acknowledgment

PLFL would like to acknowledge the support from New York Sea Grant Institute.

8 References

- [1] Fugazza, M., and L. Natale. (1992). Hydraulic design of perforated breakwaters, *J. Waterway, Port, Coastal, and Ocean Eng.*, ASCE, Vol.118, No.1, pp.1-14.

- [2] Jarlan, G. E. (1961). A perforated vertical wall breakwater, The Dock & Harbour Authority, VOL XLI, No.486, pp. 394-398.
- [3] Kakuno, S. and P.L.-F. Liu. (1992). Scattering of water waves by vertical cylinders, to be published in the J. Waterway, Port, Coastal and Ocean Engrg., ASCE.